MISSOURI S&T

CENTER FOR INFRASTRUCTURE ENGINEERING STUDIES

Strengthening of Rural Bridges Using Rapid-Installation FRP Technology

Route 63 Bridge No. H356, Phelps County

by

Dongming Yan, Ph.D.
Jianbo Li, Ph.D.
Chengling Wu
Genda Chen, Ph.D., P.E.

A University Transportation Center Program
at Missouri University of Science and Technology

Disclaimer

The contents of this report reflect the views of the author(s), who are responsible for the facts and the accuracy of information presented herein. This document is disseminated under the sponsorship of the Department of Transportation, University Transportation Centers Program and the Center for Infrastructure Engineering Studies UTC program at the Missouri University of Science and Technology, in the interest of information exchange. The U.S. Government and Center for Infrastructure Engineering Studies assumes no liability for the contents or use thereof.

Technical Report Documentation Page

1. Report No.	2. Government Accession No.	3. Recipient's Catalog No.
UTC R135		

4. Title and Subtitle	5. Report Date
Strengthening of Rural Bridges Using Rapid-Installation FRP Technology: Route 63 Bridge No. H356, Phelps County	October 2009
	6. Performing Organization Code

7. Author/s	8. Performing Organization Report No.
Dongming Yan, Ph.D., Jianbo Li, Ph.D., Chengling Wu, Genda Chen, Ph.D., P.E.	00001284

9. Performing Organization Name and Address	10. Work Unit No. (TRAIS)
Center for Infrastructure Engineering Studies/UTC program Missouri University of Science and Technology 223 Engineering Research Lab Rolla, MO 65409	11. Contract or Grant No. DTRS98-G-0021

12. Sponsoring Organization Name and Address	13. Type of Report and Period Covered
U.S. Department of Transportation Research and Innovative Technology Administration 1200 New Jersey Avenue, SE Washington, DC 20590	Final
	14. Sponsoring Agency Code

15. Supplementary Notes

16. Abstract

This report presents the use of externally bonded fiber reinforced polymers (FRP) laminates for the flexural strengthening of a concrete bridge. The bridge selected for this project is a two-span simply supported reinforced concrete slab with no transverse steel reinforcement located in Phelps County, MO. The original construction combined with the presence of very rigid parapets caused the formation of a 1-inch wide longitudinal crack, which resulted in the slab to behave as two separate elements. The structural behavior was verified using a finite element model (FEM) of the bridge. The bridge analysis was performed for maximum loads determined in accordance with AASHTO 4th edition. The strengthening scheme was designed in compliance with the ACI 440.2R-08 design guide for externally bonded FRP materials, to avoid further cracking and such that the transverse flexural capacity be higher than the cracking moment. The FRP strengthening technique was rapidly implemented. After the strengthening, a load test was performed to validate the bridge model and evaluate the structural behavior according to the AASHTO specifications. The bridge deck was retrofitted after the longitudinal crack was injected with epoxy to allow continuity in the cross section.

17. Key Words	18. Distribution Statement
Bridge, carbon fibers, FEM, fiber reinforced polymers, load test, reinforced concrete, strengthening	No restrictions. This document is available to the public through the National Technical Information Service, Springfield, Virginia 22161.

19. Security Classification (of this report)	20. Security Classification (of this page)	21. No. Of Pages	22. Price
unclassified	unclassified	32	

Form DOT F 1700.7 (8-72)

The mission of CIES is to provide leadership in research and education for solving society's problems affecting the nation's infrastructure systems. CIES is the primary conduit for communication among those on the Missouri S&T campus interested in infrastructure studies and provides coordination for collaborative efforts. CIES activities include interdisciplinary research and development with projects tailored to address needs of federal agencies, state agencies, and private industry as well as technology transfer and continuing/distance education to the engineering community and industry.

Center for Infrastructure Engineering Studies (CIES)
Missouri University of Science and Technology
223 Engineering Research Laboratory
500 West 16th Street
Rolla, MO 65409-0710
Tel: (573) 341-4497; fax -6215
E-mail: cies@mst.edu
http://www.cies.mst.edu/

RESEARCH INVESTIGATION

STRENGTHENING OF C. R. 8010 BRIDGE NO. H356, PHELPS COUNTY

PREPARED FOR THE

MERAMEC REGIONAL PLANNING COMMISSION

MISSOURI DEPARTMENT OF TRANSPORTATION

IN COOPERATION WITH THE

U.S. DEPARTMENT OF TRANSPORTATION

Written By:

Dongming Yan, Ph.D.

Jianbo Li, Ph.D.

Chenglin Wu

Genda Chen, Ph.D., P.E.

CENTER FOR INFRASTRUCTURE ENGINEERING STUDIES

MISSOURI UNIVERSITY OF SCIENCE AND TECHNOLOGY

Submitted
October 2009

STRENGTHENING OF C. R. 8010 BRIDGE NO. H356, PHELPS COUNTY

EXECUTIVE SUMMARY

This report presents the use of externally bonded fiber reinforced polymers (FRP) laminates for the flexural strengthening of a concrete bridge. The bridge selected for this project is a two-span simply supported reinforced concrete slab with no transverse steel reinforcement, located on the old 63 Highway in Phelps County, MO. The original construction combined with the presence of very rigid parapets caused the formation of a wide longitudinal crack, which resulted in the slab to behave as two separate elements. The structural behavior was verified using a finite element model of the bridge model.

The bridge analysis was performed for maximum loads determined in accordance with AASHTO Design Specifications, 4th edition, 2007. The strengthening scheme was designed in compliance with the ACI 440.2R-08 "Guide for the design and construction of externally bonded FRP systems for strengthening concrete structures", to avoid further cracking and such that the transverse flexural capacity be higher than the cracking moment. FRP strengthening technique was rapidly implemented.

The slab was retrofitted after the longitudinal major crack was injected with epoxy to allow continuity in the cross section. Once the retrofitting work was completed, a load test was performed to evaluate the effectiveness of the strengthening strategy. The structural behavior was validated by full-scale field tests.

ACKNOWLEDGMENTS

Financial support to complete this study was provided in part by the Meramec Regional Planning Commission and the Center for Infrastructure Engineering Studies, Missouri University of Science and Technology. Master Contractors installed the FRP systems, Hughes Brothers Inc. and Master Builders provided the FRP materials.

Phelps County's commissioners and staff provided the opportunity and helped in field implementation and load tests.

TABLE OF CONTENTS

LIST OF FIGURES

LIST OF TABLES

NOTATIONS

C_E	Environmental reduction factor
E_c	Longitudinal modulus of elasticity of concrete, psi
E_f	Longitudinal modulus of elasticity of the longitudinal FRP reinforcement, psi
E_s	Longitudinal modulus of elasticity of the steel reinforcement, psi
f'_c	Concrete compressive strength, psi
f^*_{fu}	Guaranteed tensile strength, ksi
f_{fu}	Design tensile strength, ks
f_y	Yield stress of the steel shear reinforcement, ksi
I_g	Gross moment of inertia of the section, in^4
I	Live load impact factor
L	Span length, ft
M_{cr}	Cracking moment of the section, kip-ft
M_n	Ultimate moment capacity, kip-ft
M_u	Design moment demand, kip-ft
P_i	Load on one wheel of the HS20-44 loading truck, kip
V_c	Concrete contribution to the shear capacity, kip
V_f	FRP reinforcement contribution to the shear capacity, kip
β_d	Modification factor based on the ratio of the modulus of the FRP reinforcement to that of steel reinforcement
ϕ	Strength reduction factor
ϕM_n	Design moment capacity, kip-ft
ε^*_{fu}	Guaranteed ultimate strain
ε_{fu}	Design ultimate strain
ρ_f	Reinforcement ratio of the FRP-reinforced section
ω_D	Total dead load, lb/ft
ω_u	Ultimate values of bending moments and shear forces, lb/ft

1 INTRODUCTION

1.1 Objectives/Technical Approach

The overall objective of this research project was to demonstrate the feasibility of externally bonding fiber reinforced polymer (FRP) reinforcement for the flexural strengthening of existing concrete bridge structures with a wide open longitudinal crack.

The bridge selected for demonstration of the FRP strengthening technology is located on County Road (C. R.) 8010, in Phelps County, Missouri (see Figure 1-1-a). This bridge was commissioned and was originally on a gravel road. Many years ago, the old Route 63 through Phelps County were concrete paved, and later it was replaced by a new 63 Highway. Commissioning of 63 Highway led to a significant decrease in traffic along C. R. 8010.

(a) Side view (b) Top view

Figure 1-1 Overview of the C. R. 8010 Bridge No. H356, Phelps County

The bridge is a two-span simply-supported reinforced concrete slab. The total bridge length is 36 ft (10.98m) and the edge-to-edge width of the bridge deck is 30 ft (9.15 m).Figure 1-2 shows a detailed geometry of the bridge. Based on the visual and Non Destructive Testing (NDT) evaluation, the bridge deck is a 9-in thick solid concrete slab with no transverse reinforcement and #10 longitudinal reinforcement bars at 6-in spacing center-to-center. From the 4 cylindrical cores (3in × 6in or 7.62cm × 15.24cm), the average compressive strength of existing concrete was measured to be 4100 psi (28.27 MPa); one reinforcement bar was tension tested to the inelastic deformation range, giving 32 ksi (220.63 MPa) in yield strength.

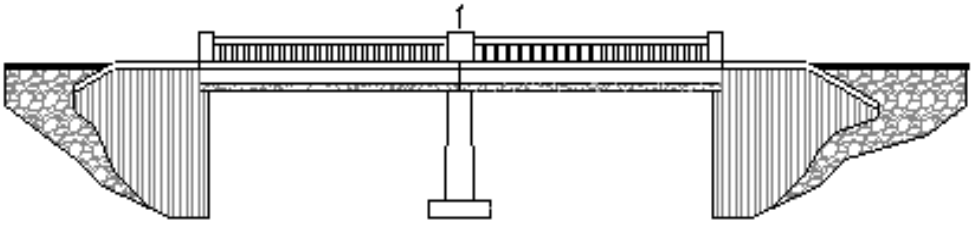

(a) Side View

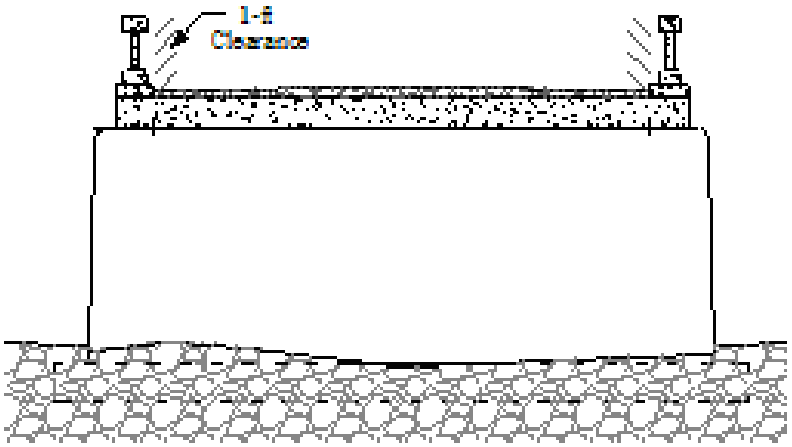

(b) Section View

Figure 1-2 C. R. 8010 Bridge Geometry

This bridge represents an ideal case for the application of FRP composites since its deficiency is due primarily to a lack of transverse reinforcing steel (Stone et al. 2002, Alkhrdaji et al. 1999, Nanni et al. 1997). Based on the initial inspection, the area where the FRP was to be installed showed excellent surface conditions. A single crack extends longitudinally through the two spans along the centerline. The crack was more than 1.0 inch (2.54 cm) wide at some locations. There was no significant cracking elsewhere and only minor corrosion of the reinforcement was detected.

This reports consisted of four major tasks:

1. Design of the required longitudinal reinforcement;
2. On-site load tests to demonstrate the effectiveness of the FRP reinforcement;
3. Field construction; and
4. Development of a Finite Element Model (FEM) of the bridge to facilitate the interpretation of the experimental data collected in the field.

1.2 Background and Significance of Work

1.2.1 FRP composites

Fiber-reinforced polymer (FRP) material systems, composed of fibers embedded in a polymeric matrix, exhibit several properties suitable for their use as structural reinforcement (Iyer and Sen 1991, JSCE Sub-Committee on Continuous Fiber Reinforcement 1992, White 1992, Neale and Labossiere 1992, Nanni 1993, Nanni and Dolan 1993, ACI Committee 440 2008, El-Badry 1996, Nanni 1997, Alkhrdaji et al. 1999, De Lorenzis et al. 2000, Nanni 2001). FRP composites are anisotropic and characterized by excellent tensile strength in the direction of the fibers. They do not exhibit yielding, but instead are elastic up to failure. FRP composites are corrosion resistant, and therefore should perform better than other construction materials in terms of weathering behavior.

1.2.2 Externally bonded repair for flexural strengthening

Structural retrofit work has come to the forefront of industry practice in response to the problem of aging infrastructure and buildings worldwide. This problem, coupled with revisions in structural codes to better accommodate natural phenomena, creates

the need for the development of successful structural retrofit technologies. The most important characteristics of repair-type work are: predominance of labor and shut-down costs as opposed to material costs, time and site constraints, long-term durability, difficulty in methodology selection and design, and effectiveness evaluation. An effective method for upgrading reinforced concrete (RC) members (prestressed and non-prestressed) is plate bonding. In Germany and Switzerland during the mid-80's, replacement of steel with FRP plates began to be viewed as a promising improvement in externally bonded repair. The advantages of FRP versus steel for the reinforcement of concrete structures include lower installation costs, improved corrosion resistance, on-site flexibility of use, and small changes in member size after repair. Of all countries, Japan has seen the largest number of field applications using bonded FRP composites (Nanni 1995).

2 NON-DESTRUCTIVE EVALUATION AND BRIDGE ANALYSIS

2.1 Non-Destructive Testing Results

Based on the visual and Non-Destructive Testing (NDT) evaluation, it was determined that the superstructure is a solid concrete slab 9 in (22.86 cm) thick, running from pier to pier. It was longitudinally reinforced with #10 (31.75 mm) bars spaced at 6 in (12.7 cm) center-to-center. No transverse reinforcement was observed. Based on the compressive tests of four cylindrical concrete cores (3in×6in or 7.62cm×15.24cm), the average compressive strength of the concrete was determined to be 4,100 psi (28.27MPa). The yield strength of the steel reinforcement was 32ksi (220.63MPa) based on the tension test of one bar.

2.2 Load Calculation Based on Non-Destructive Test Results

2.2.1 Dead load

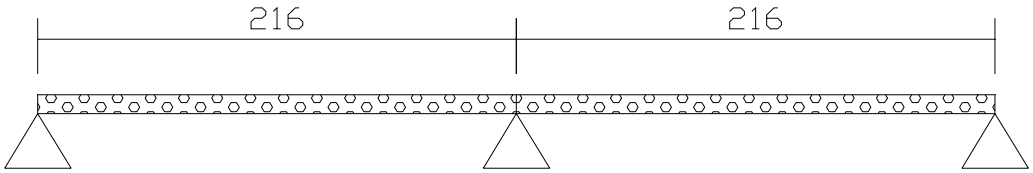

(a) Side view

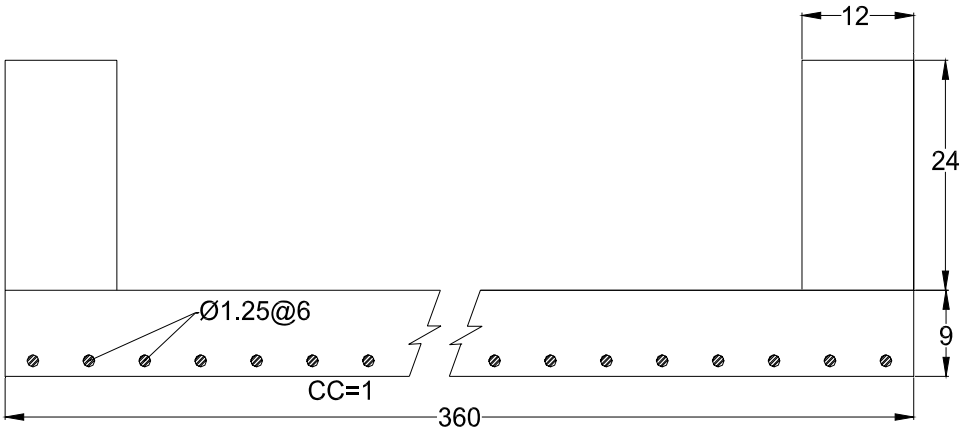

(b) Cross-section

Figure 2-1 Dimensions of the Bridge Spans and Cross Section (unit: inch)

According to AASHTO 3.5.1, the dead load shall include the weight of all components of the structure, appurtenances and utilities attached thereto, earth cover, wearing surface, future overlays, and planned widening.

In absence of more precise information, the unit weights, specified in Table 3.5.1-1, may be used for dead load. The bridge consists of two lanes. Half of the deck width was taken in calculation.

Table 2-1 Dead Load (1 k/ft = 14.7 kN/m)

Slab Weight	$\omega_{d1} = (0.15k/ft^3)(180/12\,ft)(9/12\,ft) =$	1.69	k/ft
Parapet Weight	$\omega_{d2} = (0.15k/ft^3)(12 \times 24/12^2\,ft^2) =$	0.30	k/ft
Total Dead Load	$\omega_D = \omega_{d1} + \omega_{d2} =$	1.99	k/ft

2.2.2 Live load: truck and tandem

The bridge was analyzed for a design truck load condition as shown in Figure 2-1 and for a design lane load condition. The design truck load has a front axle load of 8.0 kips, a second axle load of 32.0 kips located 14.0 ft behind the drive axle and a rear axle load also of 32.0 kips. The rear axle load is positioned at a variable distance ranging between 14.0 ft and 30.0 ft. A dynamic load allowance shall be considered as specified in Article 3.6.2.

The design tandem shall consist of a pair of 25.0 kip axles spaced 4.0 ft apart. The transverse spacing of wheels shall be taken as 6.0 ft. A dynamic load allowance shall be considered as specified in Article 3.6.2.

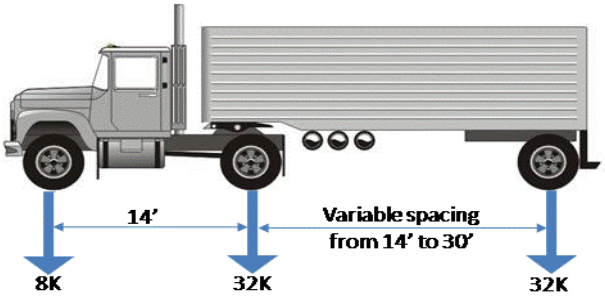

Figure 2-2 Design Truck

2.2.3 Live load: design lane load

The design lane load shall consist of a load of 0.64 k/ft uniformly distributed in the longitudinal direction. Transversely, the design lane load shall be assumed to be uniformly distributed over a 10.0-ft width. The force effects from the design lane load shall not be subjected to a dynamic load allowance (AASHTO 3.6.1.2.4).

2.2.4 Load combination

According to Eq. (3.4.1-1) in the 2007 AASHTO Design Specifications, the load combination can be expressed as

$$Q = \sum \eta_i \gamma_i Q_i$$

$$\eta_i = \frac{1}{\eta_D \eta_R \eta_I} \geq 1.0$$

η_D is a factor relating to ductility

η_R is a factor relating to redundancy

η_I is a factor relation to operational importance

The C. R. 8010 bridge represents a conventional and typical design. The level of redundancy for the bridge was assigned to be

$$\eta_D = 1.0$$

$$\eta_R = 1.0$$

$$\eta_I = 1.0$$

$\eta_{DL} = \eta_{LL} = 1.0$ for both dead load and live load

γ_i is load factors specified in Table 3.4.1-1 and 2;

$\gamma_{DL} = \gamma_p = 1.25$ for dead load;

$\gamma_{LL} = 1.75$ for live load.

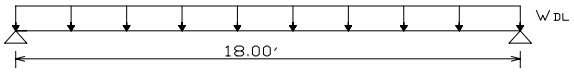

(a) Dead load

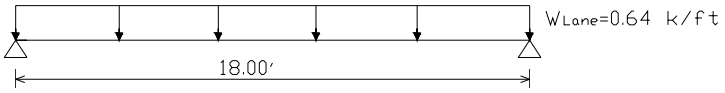

(b) Lane load

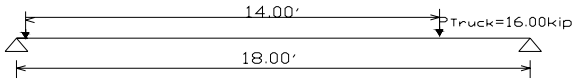

(c)Truck load

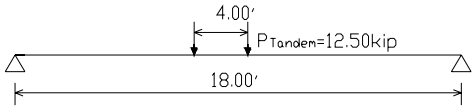

(d) Tandem load

Figure 2-3 Positions of Various Loads Applied on the Simply-supported Deck

Moment and shear force caused by the dead load:

$$M_{DL} = \frac{1}{8} w_{dl} l^2 = \frac{1}{8}(1.99k/ft)(18^2 ft^2) = 80.8 \text{ k-ft}$$

$$V_{DL} = (l - h/2) \times \omega_D / 2 = (18 - 9/12/2) \times 1.99/2 = 17.53 \text{ kip}$$

Moment and shear force caused by the design lane load:

$$M_{LA} = \frac{1}{8} w_{lane} l^2 = \frac{1}{8}(0.64k/ft)(18^2 ft^2) = 25.92 \text{ k-ft}$$

$$V_{LA} = l \times w_{lane} / 2 = 18 \times 0.64/2 = 5.76 \text{ kip}$$

The maximum moment and shear force caused by the design truck considering a variable distance from 14 ft to 30 ft between two rear axles:

$$M_{TR} = \frac{16}{2 \times 18}(18 - \frac{1}{2} \times 14)^2 = 53.78 \text{ k-ft}$$

$$V_{TR} = 16 + 16 \times \frac{4}{18} = 19.56 \text{ kip}$$

Moment and shear force caused by the Tandem:

$$M_{TD} = \frac{12.5}{2 \times 18}(18 - \frac{1}{2} \times 4)^2 = 88.89 \text{ k-ft}$$

$$V_{TD} = 12.5 + 12.5 \times \frac{14}{18} = 22.22 \text{ kip}$$

According to 3.6.1.3, the extreme force effect shall be taken as the larger of the following:

- The effect of the design tandem combined with the effect of the design lane load, or
- The effect of one design truck with the variable axle spacing between 14.0 ft and 30.0 ft.

- For both negative moment between points of contraflexure under a uniform load on all span, and reaction at interior piers only, 90 percent of the effect of two design trucks spaced a minimum of 50.0 ft. between the lead axle of one truck and the rear axle of the other truck, combined with 90 percent of the effect of the design lane load. The distance between the 32.0-kip axles of each truck shall be taken as 14.0ft.

Ultimate values of the bending moment and shear force were obtained by multiplying their nominal values by the dead and live load factors and by the impact factor:

$$\omega_u = \eta_{DL}\gamma_{DL}D + \eta_{LL}\lambda_{LL}L$$

$$M_u = 1.0\times1.25\times80.8 + 1.0\times1.75\times(25.92 + 88.89\times1.33) = 353.25\,\text{k-ft}$$

$$V_u = 1.0\times1.25\times17.53 + 1.0\times1.75\times(5.76 + 22.22\times1.33) = 83.71\,\text{kip}$$

where D is the dead load of structural components and nonstructural attachments, L is the vehicular live load, $\beta_d=1.25$ as per AASHTO Table 3.4.1-2, I=0.33 is the live load allowance based on Table 3.6.2.1-1.

2.3 Load Capacity of the Existing Bridge

2.3.1 Flexural moment capacity:

$$A_f = 30\times\frac{\pi}{4}\left(\frac{10}{8}\right)^2 = 36.8\ \text{inch}^2$$

Balance steel ratio is calculated:

$$\beta_1 = 0.85 - 0.05\frac{f_c - 4000}{1000} = 0.85 - 0.05\frac{4100 - 4000}{1000} = 0.845$$

$$\rho_b = 0.85\beta_1\frac{f_c}{f_y}\frac{87000}{87000 + f_y} = 0.85\times0.845\times\frac{4100}{32000}\times\frac{87000}{87000 + 32000} = 0.067$$

$$d = 9 - 1.0 - 1.25/2 = 7.375\ \text{in}$$

$$\rho = \frac{A_s}{bd} = \frac{36.8}{15\times12\times7.375} = 0.0278$$

Comparison between actual steel ratio of 0.0278 and the balanced steel ratio 0.067 confirms that the member is underreinforced and will fail by yielding of the steel. The depth of the equivalent stress block is found from the equilibrium condition that C=T. Hence, $0.85 f_c ab = A_s f_y$, i.e.,

$$a = \frac{A_s f_y}{0.85 f_c b} = \frac{36.8\times32{,}000}{0.85\times4100\times180} = 1.88\,\text{in}$$

By definition of a rectangular stress block, the distance to the neutral axis is

$$c = \frac{a}{\beta_1} = \frac{1.88}{0.845} = 2.22 \text{ in}$$

The ultimate moment is

$$M_n = A_s f_y (d - \frac{a}{2}) = 36.8 \times 32000 \times (7.375 - \frac{1.88}{2}) = 631.5 \text{ k-ft}$$

According to ACI 318 9.3.2,

$$\phi = 0.90$$

$$\phi M_n = 631.5 \times 0.9 = 568.3 \text{ k-ft}$$

2.3.2 Shear strength

According to ACI 318 8.6.1, for normal weight concrete,

$$\lambda = 1.0$$

According to ACI 318 11.2.1.1, for members subject to shear and flexure only,

$$V_c = 2\lambda\sqrt{f_c} b_w d = 2 \times 1.0 \times \sqrt{4100} \times 180 \times 7.375 = 170.0 \text{ kips}$$

$$\phi V_c = 170.0 \times 0.9 = 153 \text{ kips}$$

Since both ϕM_n and ϕV_n are larger than M_u and V_u respectively, no strengthening in the longitudinal direction is needed.

3 BRIDGE STRENGTHENING

The objective of the strengthening is to provide the necessary transverse reinforcement. Since no reinforcement was provided in the transverse direction, minimal strengthening is needed to ensure that the transverse design moment capacity is larger or equal to the cracking moment, in order to avoid further crack openings and deterioration of the concrete due to water percolation through the cracks.

In this study, a commercially available externally bonded Carbon Fiber Reinforced Polymers (CFRP) laminates were adopted to strengthen the bridge in the transverse direction by a manual wet lay-up installation technique. Before FRP installations, the longitudinal crack along the centerline of the bridge was first repaired in order to re-establish material continuity and assure no water percolation through the crack. For this purpose, the crack was sealed using an epoxy-paste and then injected with a very low viscosity resin as shown in Figure 3-1(a, b). FRP was then applied according to the following design provisions.

(a) Crack sealed prior to injection

(b) Crack injection underneath the bridge

Figure 3-1 Repair of Longitudinal Crack

The FRP laminates was designed according to ACI 440.2R-08, referred to ACI 440 thereafter. The properties of the FRP composite materials used in the design are summarized in Table 3-1. They are the guaranteed values by manufacturers.

The ϕ factors used to convert nominal strengths to design capacities were obtained as specified in AASHTO (2007) for the as-built bridge members and from ACI 440 for the strengthened members.

The FRP material properties reported by manufacturers, such as the ultimate tensile strength, typically do not consider long-term exposure to environmental conditions, and should be considered as initial properties. They are modified in all design equations as follows (ACI 440):

$$f_{fu} = C_E f^*_{fu}$$
$$\varepsilon_{fu} = C_E \varepsilon^*_{fu} \qquad (3.1)$$

where f_{fu} and ε_{fu} are the FRP design tensile strength and ultimate strain considering the environmental reduction factor (C_E) as given in Table 7.1 (ACI 440), and f^*_{fu} and ε^*_{fu} represent the FRP guaranteed tensile strength and ultimate strain as reported by manufacturers. The FRP design modulus of elasticity is the average value as reported by the manufacturer.

Table 3-1 Properties of CFRP Laminate Constituent Materials

Material	Ultimate Tensile Strength f^*_{fu} ksi [MPa]	Ultimate Strain ε^*_{fu} in/in [mm/mm]	Tensile Modulus E_f ksi [GPa]	Nominal Thickness t_f in [mm]
Primer*	2.5 [17.2]	40	104 [0.7]	-
Putty*	2.2 [15.2]	7.0	260 [1.8]	-
Saturant*	8.0 [55.2]	7.0	260 [1.8]	-
High Strength Carbon Fiber**	550 [3790]	0.017	33,000 [228]	0.0065 [0.1651]

* Values provided by the manufacturer (Watson Bowman Acme Corp. (2002))

** Tested as laminate with properties related to fiber area (Yang, X., 2002)

3.1 Externally Bonded CFRP Laminates

To avoid further cracking in the bridge deck, a total of five, 12 in (30.48 cm) wide, 28 ft (8.53 m) long, two-ply CFRP strips are required. The final design of the CFRP laminates was to evenly space five strips over the span length of 18 ft (5.49 m) and run the entire width of the slab, as shown in Figure 3-2. The CFRP laminates were applied by a certified contractor in accordance to manufacturer's specification (Watson Bowman Acme Corp., 2002) (see Figure 3-3).

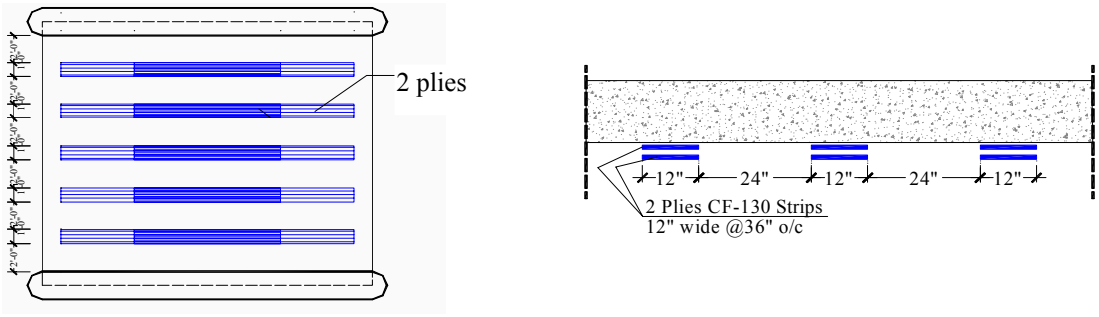

(a) Plan View (b) Section View

Figure 3-2 Strengthening with Laminates on Span 1 and 2

(a) Surface preparation with primer and putty

(b) Application of saturant

(c) Application of CFRP laminates

(d) Application completed

Figure 3-3 Phases of CFRP Laminate Installation

3.2 Field Evaluation

Although in-situ bridge load testing is recommended by AASHTO (2007) as an "effective means of evaluating the structural performance of a bridge," no guidelines currently exist for bridge load test protocols. In each case the load test objectives, load configuration, instrumentation type and placement, and analysis techniques are to be determined by the organization conducting the test.

In order to validate the behavior of the bridge, static load tests were performed with a dump truck (see Figure 3-4 and 3-5). Although different in geometry from a HS20 truck, the dump truck can create the loading configuration that maximizes the stresses and deflections at mid span just like HS20 for a short-span bridge.

Figure 3-4 Load Test with a H20 Truck

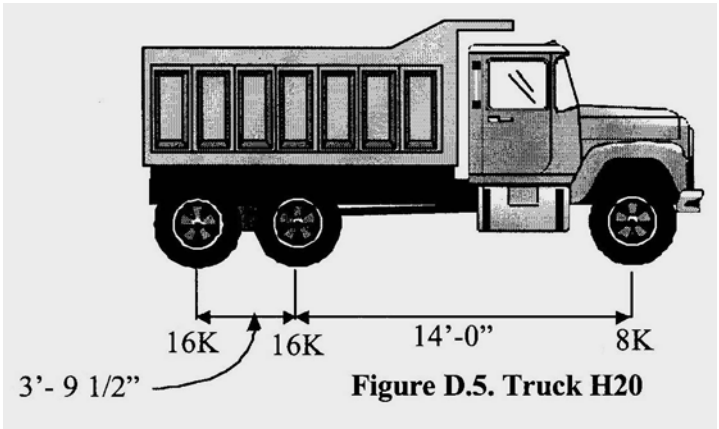

Figure 3-5 H20 Legal Truck

The bridge was tested under three passes of the truck: one central and two side passes as illustrated in Figure 3-6. For each pass, four stops were executed with the truck having its rear axle centered over the center pier, at the quarter point, at the mid-span, and over the end pier, which were clearly marked on the asphalt pavement as seen in Figure 3-7 for the side pass. During each stop, the truck stationed for at least two minutes before proceeding to the next location to allow stable readings. Vertical displacements were measured with eight Linear Variable Differential Transformers (LVDT as shown in Figure 3-8) that were distributed along the traffic direction and its perpendicular direction. The data acquisition system used for this test is shown in Figure 3-9.

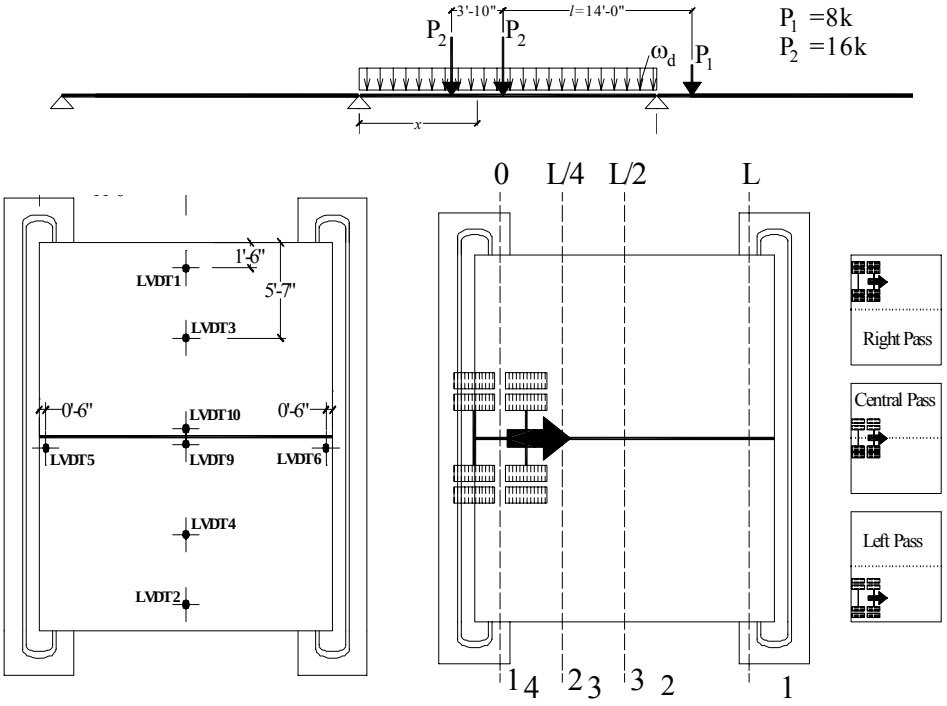

(a) Locations of LVDTs (b) Stop locations

Figure 3-6 LVDT Locations and Stop Locations of the Truck Rear Axle

Figure 3-7 Truck on the Side Pass

Figure 3-8 Installation of LVDT

Figure 3-9 Data acquisition system

The instrumentation layout was designed to understand the deflection distribution of the bridge deck. In theory, the bridge acted symmetrically. Therefore, the instrumentation system was concentrated on one half of the bridge deck. The results of the load tests are presented in Figure 3-10. These results consistently show the discontinuity of deflection along the centerline of the bridge as a result of the longitudinal crack. This was probably the first bridge application with a significant longitudinal crack. Therefore, although an effort was made to seal the crack, the two sides of the bridge deck still did not perform as one unit. Overall, the bridge performed well in terms of the maximum deflection. In fact, the maximum deflection measured during the load test is below the allowable deflection prescribed by the 2007 AASHTO, Section 8.9.3. That is $\delta_{max} \leq L/800 = 0.27$in (6.86mm).

Note that Figure 3-10, Figure 3-11 and Figure 3-12 correspond to the loading cases that the truck ran from Location 1 to 4 as marked in Figure 3-6, while Figure 3-13 and Figure 3-14 represent the truck moving from Location 4 to 1 to verify the repeatability of test data. Also note that the LVDTs along the transverse centerline were located closer to the left side. That explains why the transverse distributions of the bridge deck deflection for the left and right passes differ as illustrated in Figure 3-10 and Figure 3-12.

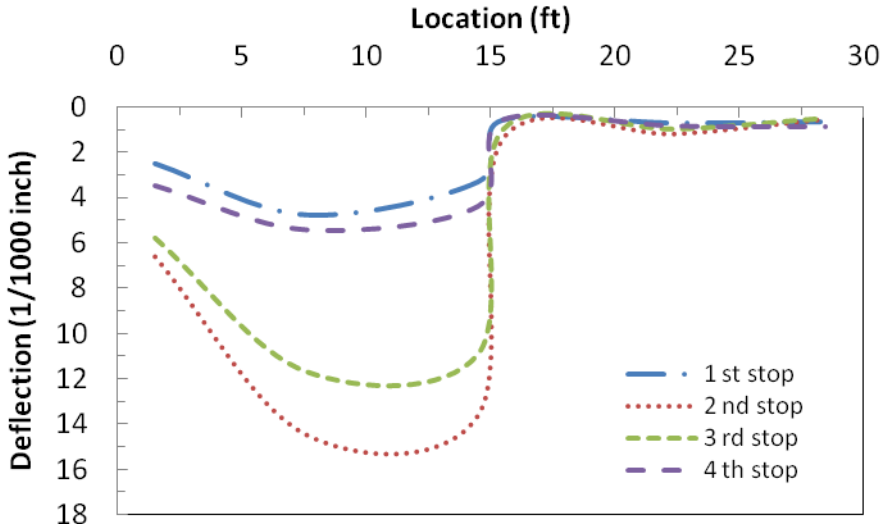

(a) Deformation along longitudinal direction

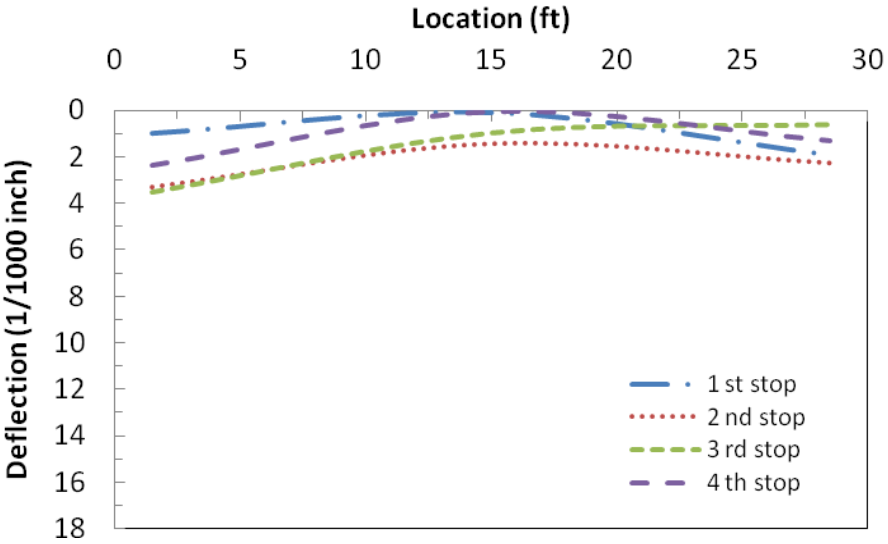

(b) Deformation along transverse direction

Figure 3-10 Deflection along the longitudinal and transverse direction (Left pass)

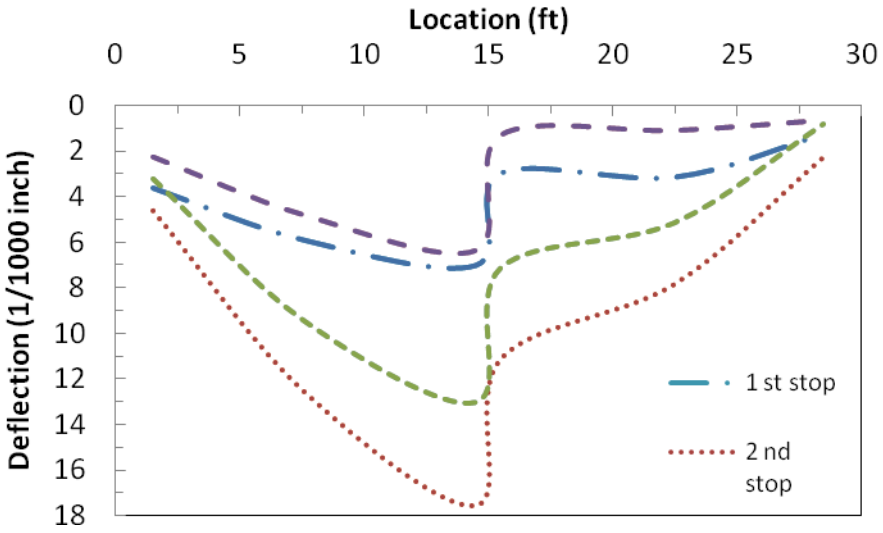

(a) Deformation along longitudinal direction

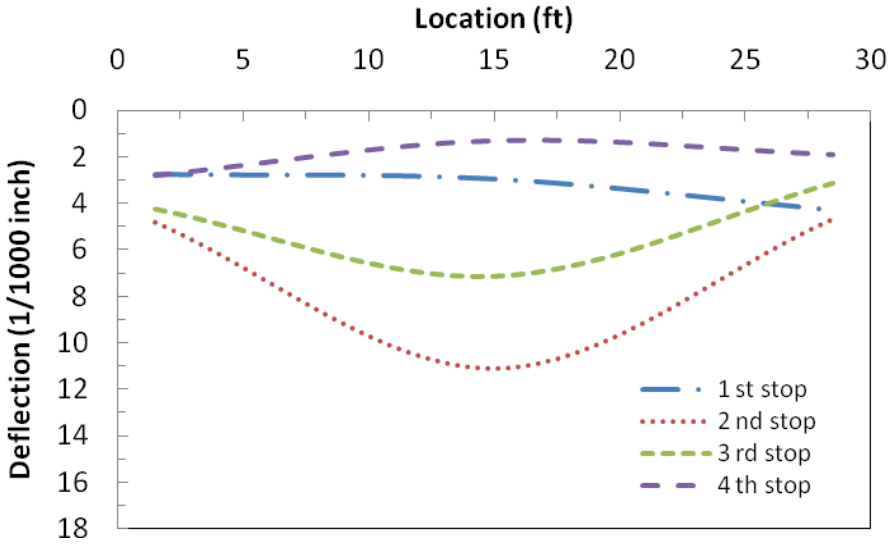

(b) Deformation along transverse direction

Figure 3-11 Deflection along the longitudinal and transverse direction (Central pass)

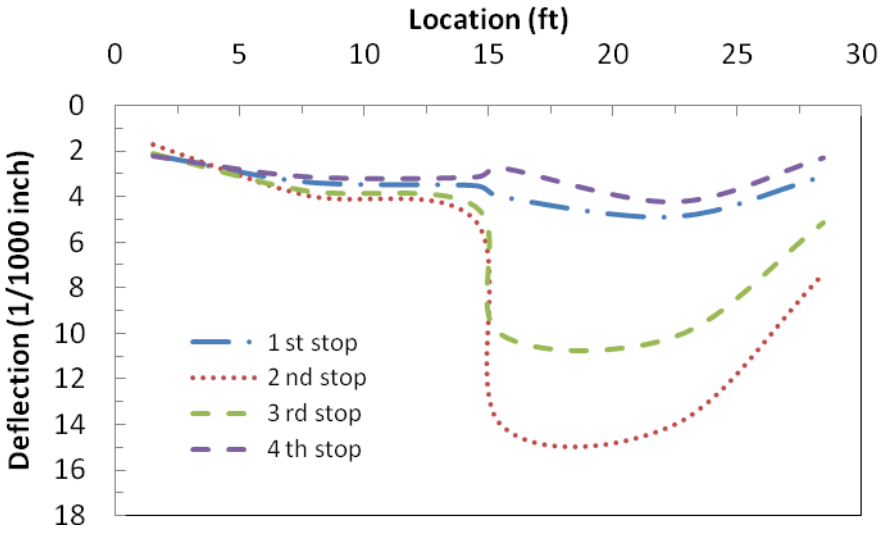

(a) Deformation along longitudinal direction

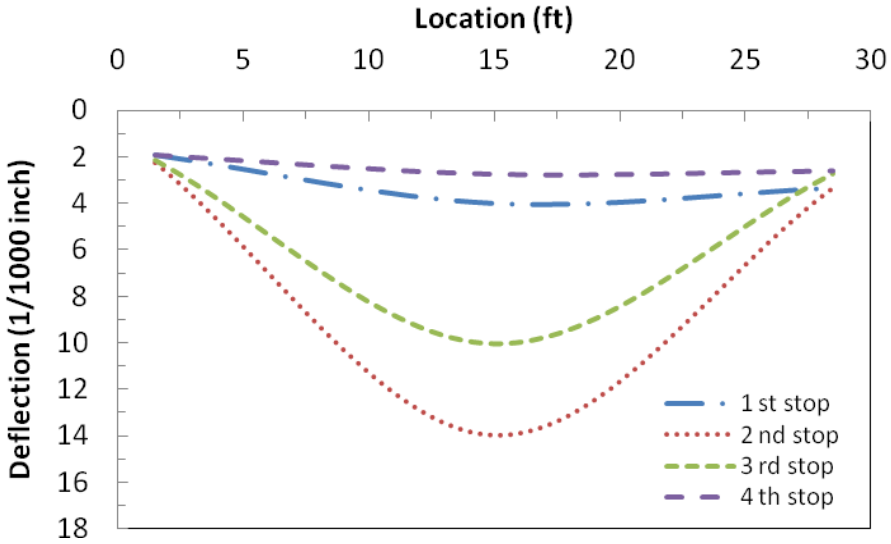

(b) Deformation along transverse direction

Figure 3-12 Deflection along the longitudinal and transverse directions (Right pass)

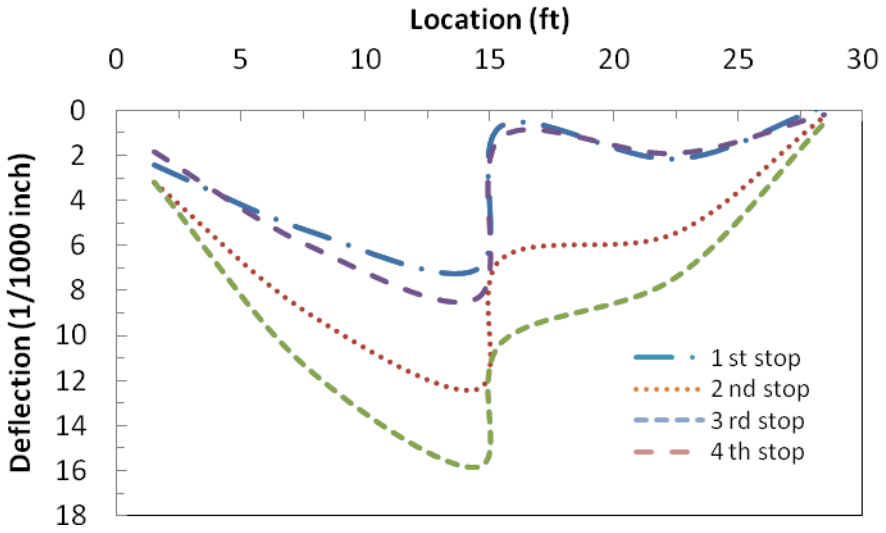

(a) Deformation along longitudinal direction

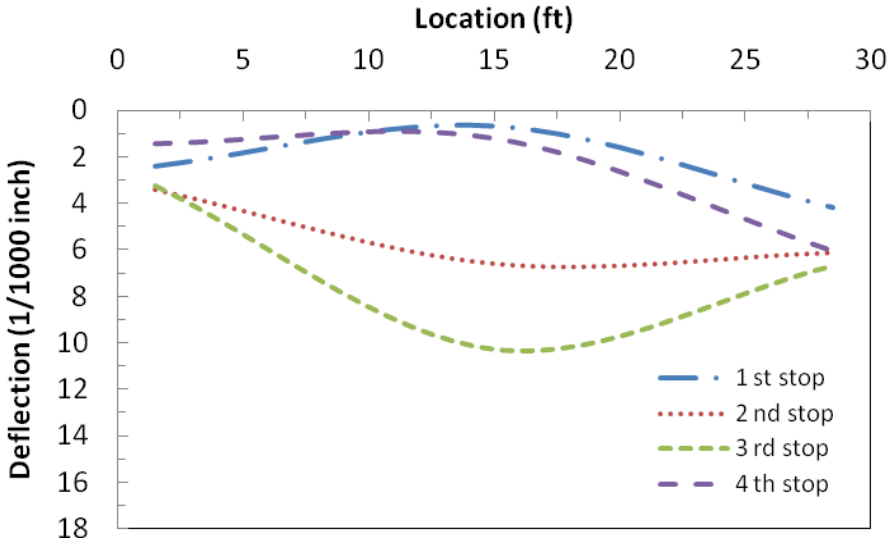

(b) Deformation along transverse direction

Figure 3-13 Deflection along the longitudinal and transverse directions (Central pass)

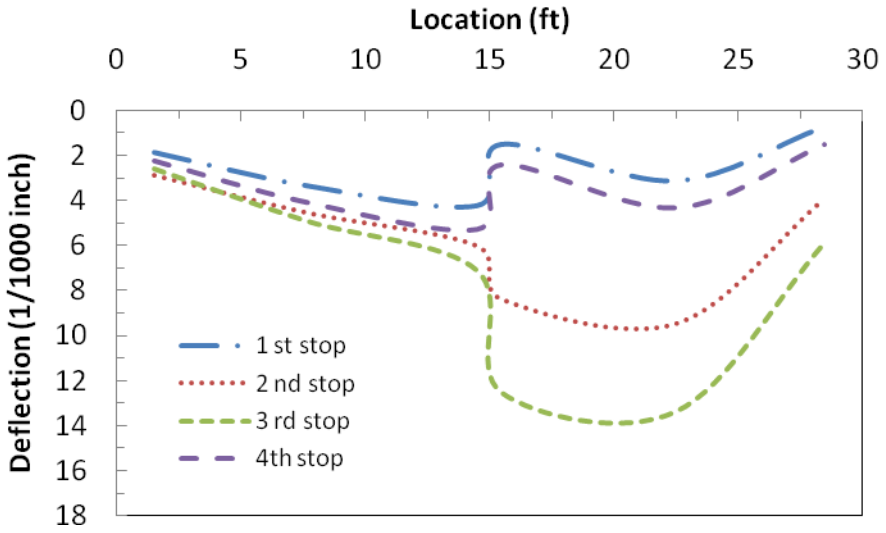

(a) Deformation along longitudinal direction

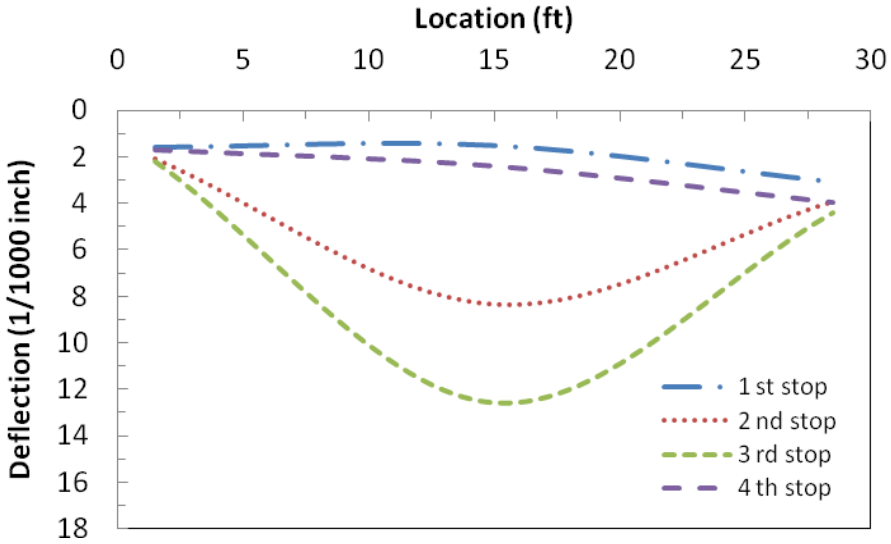

(b) Deformation along transverse direction

Figure 3-14 Deflection along the longitudinal and transverse directions (Right pass)

4 FEM ANALYSIS

To facilitate the interpretation of the test data, a linear elastic FEM of the bridge was established and analyzed using ABAQUS. An eight-node element was chosen to model the concrete deck. Each node has three translational degrees of freedom. The steel reinforcement was modeled as fiber element, which was assumed in perfect bond with the surrounding concrete. Up to three different rebar properties may be specified.

In this study, the material properties of concrete were assumed to be isotropic and linear elastic because the applied load was relatively low. The modulus of elasticity

of the concrete was based on the measured compressive strength obtained from the concrete core tests according to ACI 318-06, Section 8.5.1:

$$E_c = 57000\sqrt{f_c'} \approx 3.6\times10^6\ psi\ (24.8\ GPa)$$

Each concrete element was 3.5in × 5in × 6in (8.9cm × 12.7cm × 15.2cm). The parapet and curb on the bridge deck was modeled as an equivalent rectangular element. They were considered to be simply supported at both ends as seen in Figure 4-1 (a) and Figure 4-2 (a).

Two numerical models were developed in this study. The first numerical model (NM-I) represented the entire bridge deck with continuous plate elements that did not include the longitudinal crack observed on the bridge. The stress distribution under different loading conditions is shown in Figure 4-1 and Figure 4-2. The second model (NM-II) included the longitudinal crack by separately simulating two halves of the bridge deck. In this case, as the test truck passed on the right or left side, only the half bridge deck on that side responded to the truck load as indicated in Figure 4-3.

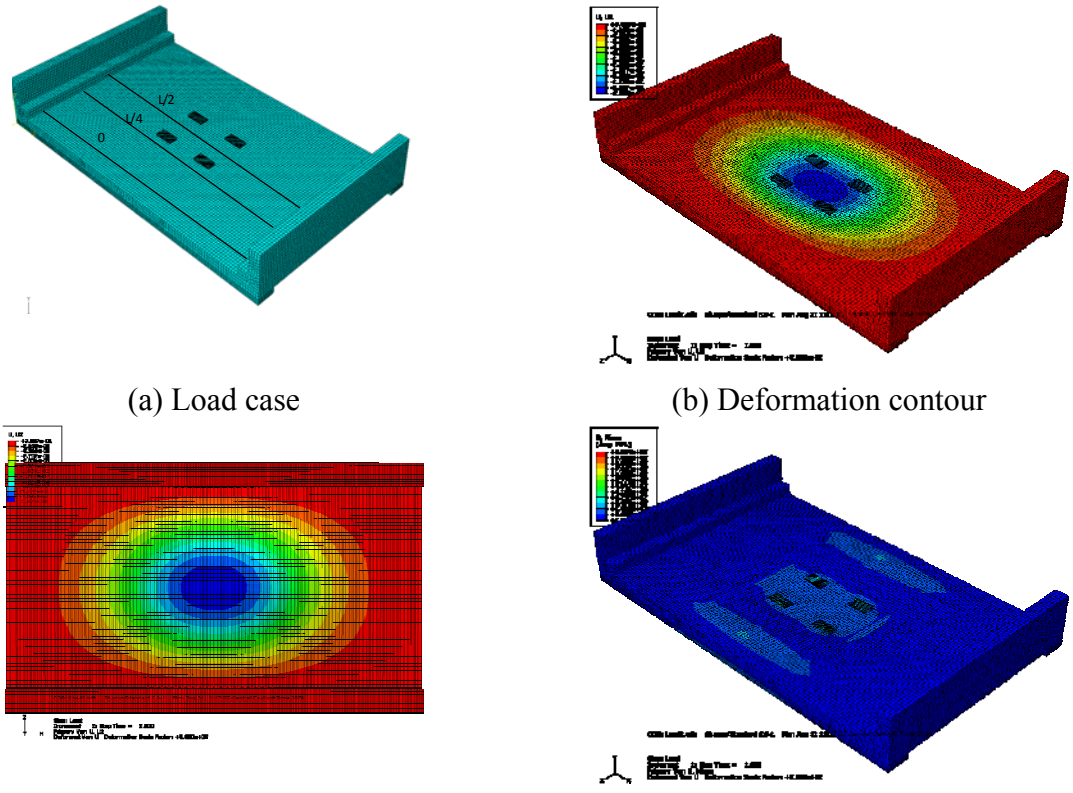

(a) Load case (b) Deformation contour

(c) Bottom view (d) Misses stress contour

Figure 4-1 Loading Case: Second Stop on Central Pass (Scale: 1:1000)

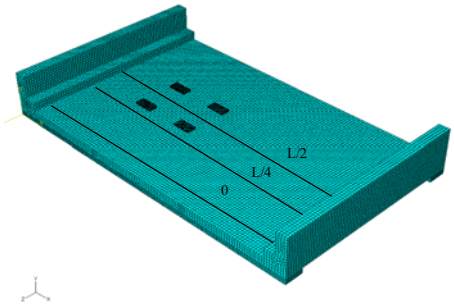

(a) Loading case

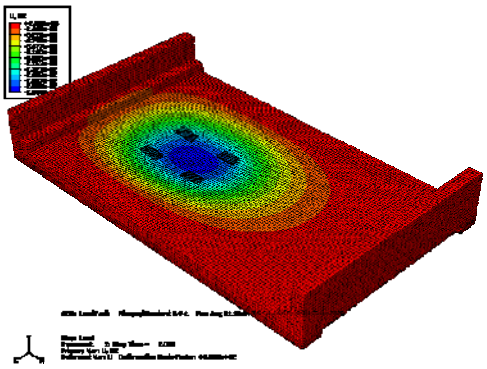

(b) Deformation contour

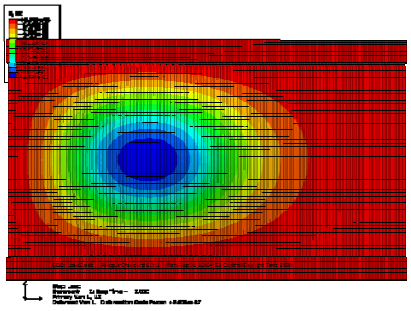

(c) Bottom view

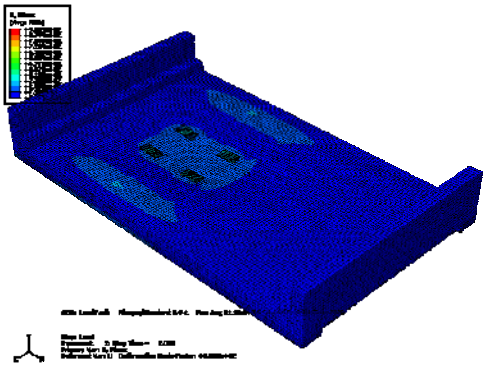

(d) Misses stress contour

Figure 4-2 Loading Case: Second Stop on Right Pass (Scale: 1:1000)

The average transverse stresses are plotted in Figure 4-1 and Figure 4-2 under both the central pass and right pass. They show how the presence of the rigid parapets has a significant effect on the overall behavior of the bridge, justifying the presence of peak horizontal stresses along the slab centerline (tensile stresses are positive) which caused the formation of the crack. The strengthening with FRP laminates can reduce the tensile stresses and guarantee a flexural capacity in the transversal direction higher than the cracking moment, preventing further cracking in the bridge deck.

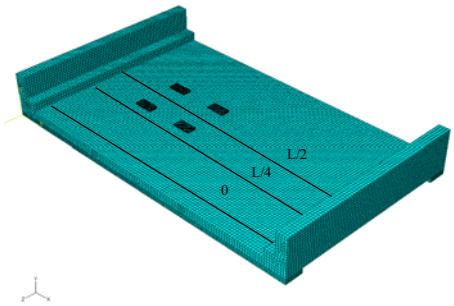

(a) Loading case

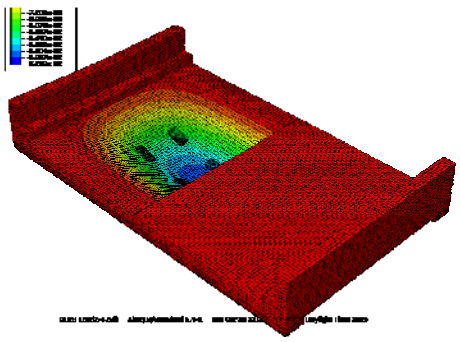

(b) Deformation contour

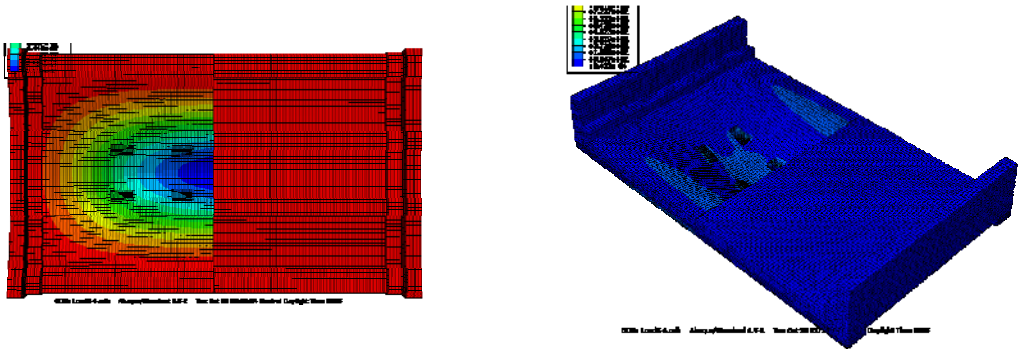

(c) Bottom view (d) Misses stress contour

Figure 4-3 Loading Case: Second Stop on Right Pass (Scale: 1:1000)

The experimental and numerical (vertical) deflections distributed along the transverse line are compared in Figure 4-4 for the central and right passes. They show a general agreement in the order of deflection. The maximum deflections obtained from the NM-I and NM-II models are respectively smaller and greater than the experimental result. This is attributable to the difference of deck stiffness in the two cases. When crack is not present, the entire bridge deck works together, experiencing a smaller deflection. When crack initiates along the centerline of the bridge deck, only half of the deck supported the truck passing on that side, resulting in a greater deflection. The lateral FRP laminate will not only restrict the further development of the crack, but also improve the integrity of the bridge deck.

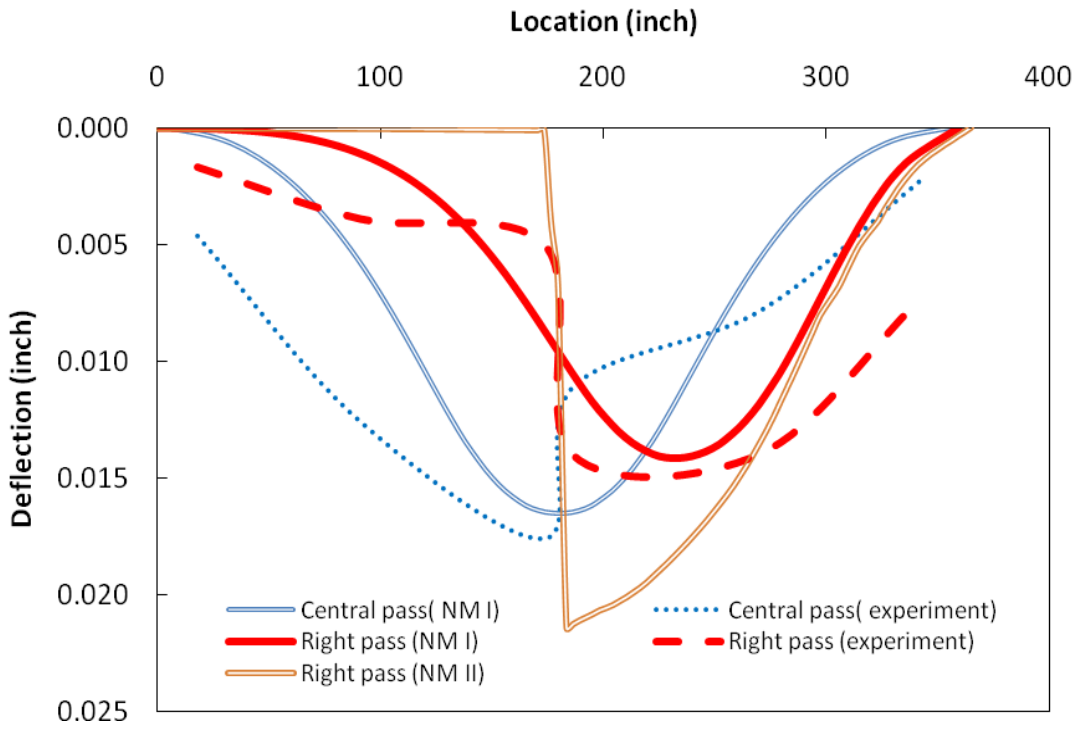

Figure 4-4 Comparison of experimental and analytical results

5 CONCLUDING REMARKS

Based on the load tests and numerical simulations, the following observations can be made:

- An externally bonded FRP laminate system is a feasible solution to upgrade the obsolete bridge to meet the current design requirement for transverse reinforcement;
- The load tests indicate that the FRP strengthening of the concrete bridge meets the deflection requirement stipulated in the 2007 AASHTO Specifications;
- The FEM analysis generally supports the field observations from load tests. The FRP laminate improve the integrity of the overall bridge deck to a certain degree, making two halves of the bridge deck partially work together. The parapet and curb of the solid slab bridge significantly contribute to the overall stiffness of the bridge system.

6 REFERENCES

AASHTO (2007): "Standard Specifications for Highway Bridges", 17th Edition, Published by the American Association of State Highway and Transportation Officials, Washington D.C.

ACI 440.2R-08, 2008: "Guide for the Design and Construction of Externally Bonded FRP Systems for Strengthening Concrete Structures," Published by the American Concrete Institute, Farmington Hills, MI.

ACI 318-02, 2002: "Building Code Requirements for Structural Concrete and Commentary (318R-02)," Published by the American Concrete Institute, Farmington Hills, MI.

Alkhrdaji, T., Nanni, A., Chen, G., and Barker, M. (1999), "Upgrading the Transportation Infrastructure: Solid RC Decks Strengthened with FRP," Concrete International, American Concrete Institute, Vol. 21, No. 10, October, pp. 37-41.

ANSYS User's Manual for Revision 6.1 (2000): Volume I Procedure and Volume III Elements, Swanson Analysis Systems, Inc.

De Lorenzis, L. (2002), "Strengthening of RC Structures with Near Surface Mounted FRP Rods", Ph.D. Thesis, Department of Innovation Engineering, University of Lecce, Italy, 289 pp. http://nt-lab-ambiente.unile.it/delorenzis.

De Lorenzis L., Nanni A., and La Tegola A. (2000), "Flexural and Shear Strengthening of Reinforced Concrete Structures with Near Surface Mounted FRP

Rods," Proceedings of Third International Conference on Advanced Composite Materials in Bridges and Structures, Ottawa, Canada, August, pp. 521-528.

El-Badry, M. (1996), "Advanced Composite Materials in Bridges and Structures," Proceedings ACMBS-II, Montreal, Canada, pp. 1027.

Hughes Brothers, Inc. (2002), Aslan® 500 CFRP Tape, http://www.hughesbros.com

Iyer, S.L. and R. Sen, Editors (1991), "Advanced Composite Materials in Civil Engineering Structures," Proc., American Society of Civil Engineers, New York, NY, 443 pp.

JSCE Sub-Committee on Continuous Fiber Reinforcement (1992), "Utilization of FRP-Rods for Concrete Reinforcement," Proc., Japan Society of Civil Engineers, Tokyo, Japan, 314 pp.

Nanni, A., Ed. (1993), Fiber-Reinforced-Plastic (FRP) Reinforcement for Concrete Structures: Properties and Applications, Developments in Civil Engineering, Vol. 42, Elsevier, Amsterdam, The Netherlands, pp. 450.

Nanni, A. and Dolan, C.W., Eds. (1993), "FRP Reinforcement for Concrete Structures," Proc., ACI SP-138, American Concrete Institute, Detroit, MI, pp. 977.

Nanni, A., (1995)."Concrete Repair with Externally Bonded FRP Reinforcement: Examples from Japan," Concrete International: Design and Construction, Vol. 17, No. 6, June 1995, pp. 22-25.

Nanni, A., (1997), "Carbon FRP Strengthening: New Technology Becomes Mainstream," Concrete International: Design and Construction, V. 19, No. 6, pp. 19-23

Nanni, A. (2001), "Relevant Applications of FRP Composites in Concrete Structures," Proc., CCC 2001, Composites in Construction, Porto, Portugal, Oct. 10-12, 2001, J Figueiras, L. Juvandes and R. Furia, Eds., (invited), pp. 661-670.

Neale, K.W. and Labossiere, P., Editors (1992), "Advanced Composite Materials in Bridges and Structures," Proc., Canadian Society for Civil Engineering, Montreal, Canada, 705 pp.

Stone, D.K., Tumialan, J.G., Parretti, R., and Nanni, A., (2002). "Near-Surface Mounted FRP Reinforcement: Application of an Emerging Technology", Concrete UK, V. 36, No. 5, pp. 42-44.

Watson Bowman Acme Corp. (2002), Wabo®MBrace Composite Strengthening System Design Guide, Third Edition, Amherst, New York.

White, T.D., Editor (1992), "Composite Materials and Structural Plastics in Civil Engineering Construction," in Proc. of The Materials Engineering Congress, American Society of Civil Engineers, New York, NY, pp. 532-718.

Yang, X. (2001), " The engineering of construction specifications for externally bonded FRP composites" Doctoral Dissertation, Department of Civil Engineering, University of Missouri-Rolla, Rolla, Missouri, 166 pp.